Journal of Materials Science & Nanotechnology
Volume 5 | Issue 2
ISSN: 2348-9812

Research Article Open Access

Biological Effect Tetra-Branched Anti-TNF-Peptide and Coating Ratio-Dependent Penetration of the Peptide-Conjugated Cerium$^{3/4+}$ Cation-Stabilized Gamma-Maghemite Nanoparticles into Rat Inner Ear after Transtympanic Injection Visualized By MRI

Zou J[*1,3], Peng B[#2], Ostrovsky S[#4], Li B[2], Li C[2], Kettunen MI[5], Lellouche JP[4], and Pyykkö I[3]

[1]Department of Otolaryngology-Head and Neck Surgery, Center for Otolaryngology-Head & Neck Surgery of Chinese PLA, Changhai Hospital, Second Military Medical University, Shanghai, China
[2]Hebei Bio-high Technology Deve CO., LTD, Shijiazhuang, Hebei Province, China
[3]Hearing and Balance Research Unit, Field of Oto-laryngology, School of Medicine, University of Tampere, Tampere, Finland
[4]Laboratory of Nanoscale Materials and Systems, Department of Chemistry, Bar-Ilan University, Ramat-Gan, Israel
[5]A.I. Virtanen Institute for Molecular Sciences, University of Eastern Finland, Kuopio, Finland
[#]Both authors contributed equally

[*]**Corresponding author:** Zou J, Department of Otolaryngology-Head and Neck Surgery, Center for Otolaryngology-Head & Neck Surgery of Chinese PLA, Changhai Hospital, Second Military Medical University, Shanghai, China, Hearing and Balance Research Unit, Field of Oto-laryngology, School of Medicine, University of Tampere, Tampere, Finland, Tel: +86 21 311 62021, E-mail: Jing.Zou@staff.uta.fi

Citation: Zou J, Peng B, Ostrovsky S, Li B, Li C, et al. (2017) Biological Effect Tetra-Branched Anti-TNF-Peptide and Coating Ratio-Dependent Penetration of the Peptide-Conjugated Cerium$^{3/4+}$ Cation-Stabilized Gamma-Maghemite Nanoparticles into Rat Inner Ear after Transtympanic Injection Visualized By MRI. J Mater Sci Nanotechnol 5(2): 204

Received Date: August 23, 2017 **Accepted Date:** October 25, 2017 **Published Date:** October 28, 2017

Abstract

Objective: To evaluate the biological efficacy of TBATP and their distribution in the inner ear after transtympanic injection.

Methods: TBATP was synthesized through standard Fmoc solid phase synthesis. A model of TNF-α-induced apoptosis was established in human umbilical vein endothelial cells (HUVECs). The peptides were covalently attached onto CAN-γ-Fe_2O_3 NPs. Nanoparticle suspension was injected to rat middle ear cavity. Distribution of CAN-γ-Fe_2O_3 NPs in the inner ear was detected using a 7.0 T MRI machine in combination with Prussian blue staining.

Results: TBATP almost fully suppressed the inhibitory effect on HUVECs induced by TNF-α while the linear one reduced less than half of the effect. CAN-γ-Fe_2O_3 NPs conjugated to TBATP at a peptide weight ratio of 10% but not 50% efficiently entered the inner ear at 3 h through 2 w post-middle ear administrations and most pronounced at 2 w.

Conclusion: The tetra-branched anti-TNF-α peptide (TBATP) is capable of suppressing the inhibitory effect on HUVECs induced by TNF-α, and is visualized by MRI after conjugating to super-paramagnetic $Ce^{3/4+}$ cation-doped maghemite nanoparticles arising from ceric ammonium nitrate-mediated doping oxidation of starting magnetite nanoparticles (CAN-γ-Fe_2O_3 NPs).

Keywords: Peptide; Functional maghemite nanoparticles; Inner ear; Magnetic resonance imaging; Biological barrier

List of Abbreviations: CAN-γ-Fe_2O_3 NPs: Super-paramagnetic maghemite (γ-Fe_2O_3) nanoparticles using ceric ammonium nitrate (CAN)-mediated oxidation of starting magnetite (Fe_3O_4) nanoparticles; HUVECs: Human umbilical vein endothelial cells; TNF-α: tumor necrosis factor-α

Introduction

The cascades of tumor necrosis factor-α (TNF-α) have been implicated in the pathological progress of noise induced hearing loss, sudden sensorineural hearing loss, age related hearing loss, and neonatal hyperbilirubinaemia induce neural toxicity [1-6]. Application of TNF-α blocker (antibody) has been reported to improve the auditory function in noise induced hearing loss,

autoimmune sensorineural hearing loss [7-9]. However, antibodies against TNF-α have too large molecular weight to access the therapeutic target. Peptides are smaller in size, more stable during storage, and easier to manipulate than antibodies. To simulate antibody in structure, novel tetra-branched anti-TNF-α peptide selected using phage library with capability of inhibiting human TNF-α binding to its receptors were developed [10]. It is clinically relevant to develop a similar therapeutics for treating the inner ear diseases.

The intratympanic delivery of therapeutics is a currently used approach in clinical practice with advantages of avoiding systemic adverse effects and reducing the administration dosage to the individual. *In vivo* MRI studies demonstrated that intratympanic delivery induced more gadolinium chelate passage into the perimodiolar lymph and lateral wall of mouse cochlea than did the intravenous injection attributed to potential porous structures of medial wall of the scala tympani and spiral ligament extracellular space [11]. An efficient passage of agents into the modiolus and lateral wall would raise the possibility that drug delivery to these areas of the cochlea might be favored by intratympanic route. *In vivo* tracking distribution of therapeutics in the targeting organ is a reliable method to follow the dynamics of the delivered agents. We recently disclosed the preparation of highly hydrophilic anti-aggregative super-paramagnetic maghemite (γ-Fe_2O_3) nanoparticles (NPs) using ceric ammonium nitrate (CAN)-mediated oxidation of starting magnetite (Fe_3O_4) NPs (CAN-γ-Fe_2O_3 NPs), which were highly stable aqueous suspensions/ferrofluids due to a unique ultrasound-mediated doping process of the Fe_3O_4 NP surface using lanthanide $Ce^{3/4+}$ cations [12]. We have also demonstrated that the novel CAN-γ-Fe_2O_3 NPs is a strong T_2 MRI contrast agent and penetrats both round and oval windows, which has potential application in the molecular imaging of the inner ear [13].

The present study aimed to develop feasible agents for the inner ear therapy as well as diagnosis, and acquire information about their passing through the round and oval windows after conjugation with MRI-traceable nanoparticles. Tetra-branched anti-TNF-α peptides were developed according to a previous report with modifications [10]. Biological effect of the peptides in inhibiting TNF-α induced cellular impairment was analyzed in cell cultures. The specific peptides were conjugated to CAN–γ-Fe_2O_3 NPs at various ratios and the resulting dynamic distributions in the inner ear after middle ear administration have been evaluated in rats using *in vivo* MRI.

Materials and Methods

Synthesization and Characterization of Tetra-Branched Anti-TNF-α Peptide

The sequences of effective peptide were HIHDDLLRYYGW, and that of scramble peptide were HDYLHRILGYDW. The selected peptides were synthesized in a tetrameric form (Figure 1) through standard Fmoc solid phase synthesis, building the tetramer on a three-lysine core and polyethylene glycol tail [10]. The synthesis was performed on a Sophas P1 S Solid Phase Peptide Synthesizer (Zinsser Analytic GmbH, Frankfurt, Germany) using [Fmoc-Lys(Fmoc)]2-Lys-βAla-2Cl Resin (0.15 mmol/g) (Shanghai Top-Peptide Biotechnology Co. Ltd., Shanghai, China), Fmoc-amino acids (0.5 mol/L), 2-(1H-benzotriazol-1-yl)-1,1,3,3-tetramethyluronium hexafluorophosphate (0.25 mol/L), *N,N*-Diisopropylethylamine (0.3 mol/L) (GL Biochem Co. Ltd., Shanghai, China) through rinse, deprotection, and ligase circles.

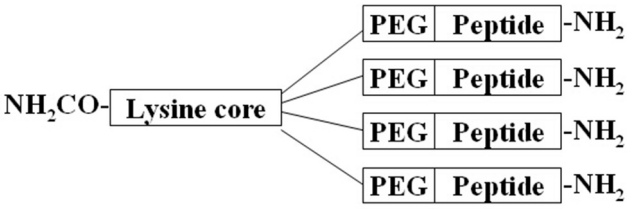

Figure 1: Schema of the tetra-branched peptides

For characterization, the peptide-resin complexes were pyrolyzed at room temperature for 3 h in the following solutions, trifluoroacetic acid: 3-hydroxytoluene: thioanisole: H_2O: ethane-1,2-dithiol=82.5: 5: 5: 5: 2.5. After removing the resin through filtration, the peptides were sedimentated using ice ether, centrifugated at 2362.5 g (4 °C) for 7 times, and then lyophilized. The samples (1 mg/mL, 50 μl) were run on an Agilent HPLC 1100 equipped with a column of Agilent 300SB-C18 4.6*250mm. The mobile phase A was composed of 0.1% trifluoroacetic acid in H_2O, and mobile phase B was composed of 0.1% trifluoroacetic acid in acetonitrile. The elution gradient was created by mixing A and B at various ratio at different time points. B: A=1/4, 2/3, 3/2, 9/1, and 1/4 at 0, 15, 25, 30, and 35 min. 5μm (Agilent Technologies, California, USA) at an elution speed of 1.0 mL/min and temperature of 40 °C.

Impact of Tetra-Branched Anti-TNF-α Peptide on Cellular Toxicity Induced by TNF-α

Firstly, a cellular model of apoptosis was established in human umbilical vein endothelial cells (HUVECs) using TNF-α (Supplementary material 1). After optimization with concentrations of TNF-α for establishing the cell model of apoptosis in HUVECs, the impact of tetra-branched anti-TNF-α peptide on cellular toxicity induced by TNF-α was then analyzed. HUVECs were cultivated as above mentioned. When the cells propagated for 24 h and formed a monolayer confluent, 100 μL of the following

solutions were added to each well with 6 repeats. **A.** Negative control without any treatment; **B.** TNF-α (40 ng/mL)+tetra-branched anti-TNF-α peptide (0 μg/ mL); **C.** TNF-α (40 ng/mL)+tetra-branched anti-TNF-α peptide (25 μg/ mL); **D.** TNF-α (40 ng/ mL)+tetra-branched anti-TNF-α peptide (50 μg/ mL); **E.** TNF-α (40 ng/mL)+tetra-branched anti-TNF-α peptide (100 μg/ mL); **F.** TNF-α (40 ng/mL)+tetra-branched anti-TNF-α peptide (200 μg/ mL); **G.** TNF-α (40 ng/mL)+tetra-branched anti-TNF-α peptide (400 μg/ mL). The baseline reference and MTT assay were performed as above mentioned.

After optimization with concentrations for inhibiting apoptosis in HUVECs, intervention effect of tetra-branched anti-TNF-α peptide was compared with that of tetra-branched scrambled peptides, linear specific anti-TNF-α peptide, and linear scrambled peptides. HUVECs were cultivated as above mentioned. When the cells propagated for 24 h and formed a monolayer confluent, 100 μL of the following solutions were added to each well with 6 repeats. **A.** Negative control without any treatment; **B.** TNF-α (40 ng/mL); **C.** TNF-α (40 ng/mL)+tetra-branched anti-TNF-α peptide (200 μg/ mL); **D.** TNF-α (40 ng/mL)+tetra-branched scrambled peptides (200 μg/ mL); **E.** TNF-α (40 ng/mL)+linear anti-TNF-α peptide (800 μg/ mL); **F.** TNF-α (40 ng/mL)+linear scrambled peptides (800 μg/ mL). The baseline reference MTT assays were performed as described in Supplementary material 1.

Preparation and Characterization of Tetra-Branched anti-TNF-α-Peptide-Conjugated CAN-γ-Fe_2O_3 NPs

All the specific chemicals and reagents (analytical grade and/or highest purity level) used in this study, i.e., $FeCl_3 \bullet 6H_2O$, $FeCl_2 \bullet 4H_2O$, NH_4OH (ACS reagent, 28-30%), ceric ammonium nitrate (CAN, $CeIV(NH_4)_2(NO_3)_6$) have been purchased from Sigma-Aldrich (Israel) and have been used without any further purification. Starting neat neutral magnetite (Fe_3O_4) nanoparticles (Fe_3O_4 NPs, basic Massart hydrolytic method) were prepared as nanocarrier (Supplementary material 2).

Experimental Procedure for Nanocarrier Fabrication with Tetra-Branched Anti-TNF-α-Peptide Covalent Attachment to CAN-γ-Fe_2O_3 NPs

Corresponding CAN-γ-Fe_2O_3 NPs aqueous suspension (1 mL, Fe=1.96 mg/mL –ICP-AES measurement) was diluted to 25.0 mL using milliQ-purified H_2O. Then, 0.196 mg and 0.98 mg of tetra-branched anti-TNF-α peptide (peptide/Fe Wt ratio: 10% and 50% respectively) were added to the NP suspension as an aqueous solution and the medium was shaken overnight at 15 °C (orbital shaker). At completion of peptide contacting/NP surface decoration, resulting tetra-branched anti-TNF-α $peptide_{10\%}$ - CAN-γ-Fe_2O_3 NPs and tetra-branched anti-TNF-α $peptide_{50\%}$ -CAN-γ-Fe_2O_3 were washed 3 times (3 x 10 mL ddH_2O) using an Amicon® Ultra-15 centrifugal filter device (100K) operated at 4,000 rpm (5 min) to afford cleaned tetra-branched anti-TNF-α $peptide_{10\%}$ -CAN-γ-Fe_2O_3 and tetra-branched anti-TNF-α $peptide_{50\%}$ -CAN-γ-Fe_2O_3 NPs. Covalent contact of tetra-branched anti-TNF-α peptide (10% and 50% wt ratio) with CAN-γ-Fe_2O_3 NPs procedure was performed as discussed above.

Middle Ear Administration of Tetra-Branched Anti-TNF-α-Peptide-Conjugated CAN–γ-Fe_2O_3 NPs and MRI of Rat Inner Ear

Four male Sprague Dawley rats (8 ears), weighing between 300 and 350 grams, were maintained in the animal laboratory of A.I. Virtanen Institute for Molecular Sciences, University of Eastern Finland. The animals were randomly assigned into 2 groups (NP10, NP-50) (Table 1). The left ear was utilized for the delivery, and the right side was used as a negative control (NC group in Table 1). All the animal experiments have been approved by the Ethical Committee of University of Tampere (permission: ESAVI/3033/04.10.03/2011). Animal care and experimental procedures were conducted in accordance with European legislation. Throughout the experiments, the animals were anesthetized with a 5% isoflurane–oxygen mixture (flow-rate 1.0 L/min) for induction and a 2% isoflurane–oxygen mixture for maintenance *via* a facemask. Intramuscular injection of enrofloxacin (Baytril®vet, Orion, Turku, Finland) at a dose of 10 mg/kg was applied before the intratympanic administration of NPs to prevent potential infection. The animal's eyes were protected with Viscotears® (Novartis Healthcare A/S, Copenhagen, Denmark). The peptide-conjugated CAN-γ-Fe2O3 NPs were administered to the middle ear cavity with an injection tube by touching the surface of the tympanic medial wall according to a previously reported procedure [13,14]. A total volume of 10 μL of undiluted CAN-γ-Fe2O3 NP suspension was injected onto the medial wall of the middle ear cavity. The animals remained in the lateral position with the injected ear upward for 15 min before MRI study. After the last MRI measurement, the animals were decapitated for Prussian blue staining for iron in the tissue (Supplementary material 3) (Table 1).

Measurements	Number of ears		
	NP-10	NP-50	NC
MRI	2	2	4*
Prussian blue Staining	2	2	4*

MRI studies were performed at the time points of 3 h, 1 d, and 2 w post-middle ear administrations. **NC**: negative control; **NP-10**: CAN-γ-Fe_2O_3 NPs were conjugated to tetra-branched anti-TNF-α-peptide at 10% peptide ratio; **NP-50:** CAN-γ-Fe_2O_3 NPs were conjugated to tetra-branched anti-TNF-α peptide at 50% peptide ratio. *The right ear of each animal was used as **NC** in all studies.

Table 1: Assignments of rat ears in MRI measurements and histology post-middle ear administration of tetra-branched anti-TNF-α-peptide-conjugated CAN-γ-Fe_2O_3 NPs

Statistics

In cell culture study, inhibition ratios on cell viability by different treatments were compared using one-way analysis of variance. Values of $p<0.05$ were accepted as statistically significant.

Results

Characterization of Tetra-Branched Anti-TNF-α Peptide and the Inhibiting Effect on Apoptosis of HUVECs Induced By TNF-α

Purity of both tetra-branched anti-TNF-α and scramble peptides was approved by high performance liquid chromatography that demonstrated the unique specific peak of the peptides (Figure 2). The other sharp peaks might be associated with incomplete cracking of the protecting group for the side chain according to experience. A cell model of apoptosis was successfully established in HUVECs using TNF-α, which showed inhibition on viability of the cells after 24 h incubation in a concentration-dependent response. TNF-α protein at 40 ng/mL induced an average apoptosis of 30.1% of the cells and was selected as the optimized concentration for the following experiments (Figure 3A). Tetra-branched anti-TNF-α peptide suppressed the inhibitory effect on HUVECs induced by TNF-α in a dosage-dependent reaction, and 200 μg/mL of the peptides demonstrated the maximum effect of 69.2% that was used for comparison with other peptides in the following study (Figure 3B). The linear anti-TNF-α peptide also suppressed the inhibitory effect on HUVECs induced by TNF-α but significant lower than did the tetra-branched anti-TNF-α peptide (Figure 3C).

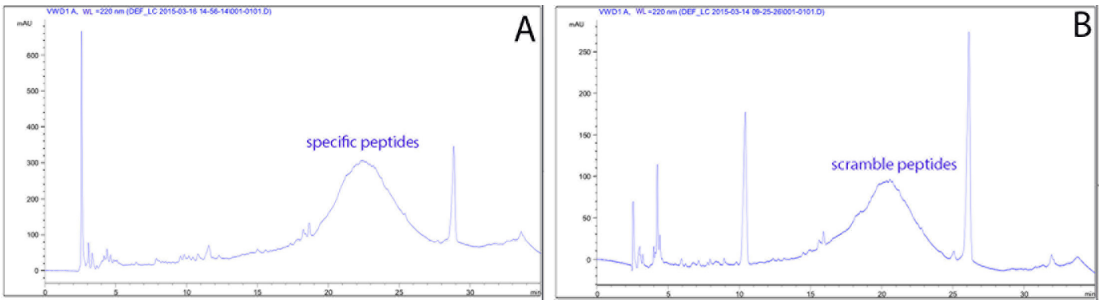

Figure 2: High performance liquid chromatography of tetra-branched anti-TNF-α peptide. The unique peak corresponds to either the specific peptides (A) or scramble peptides (B). The other sharp peaks might be associated with incomplete cracking of the protecting group for the side chain

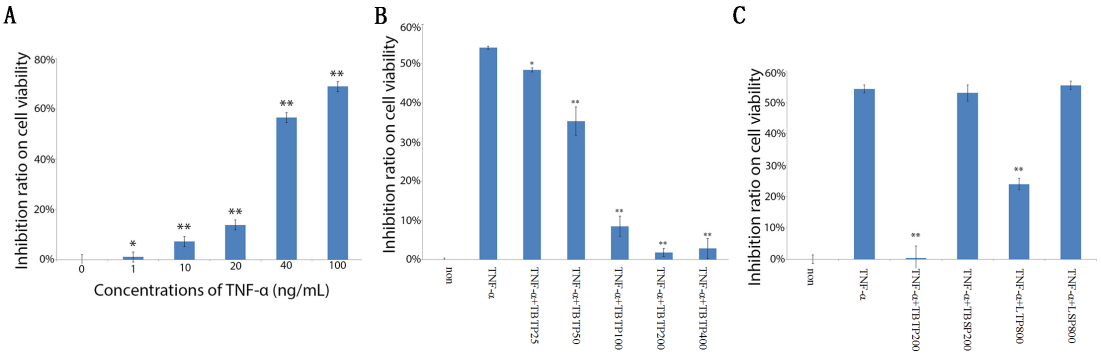

Figure 3: TNF-α-induced human umbilical vein endothelial cell death and intervention effect of anti-TNF peptides. **A.** Dose response of inhibition on viability of human umbilical vein endothelial cells induced by TNF-α. **B.** Dose response of tetra-branched TNF peptides on inhibitory effect of TNF-α in human umbilical vein endothelial cells. **C.** Impacts of various tetra-branched peptides on inhibitory effect of TNF-α in human umbilical vein endothelial cells. MTT assay was applied to evaluate the inhibitory effect. *$p<0.05$; **$p<0.01$ (one-way analysis of variance comparing to group 0 in A or group TNF-α in **B** and **C**). TNF-α+LSP800: cells were treated with TNF-α (40 ng/mL) plus linear scramble peptides (800 μg/mL); TNF-α+LTP800: TNF-α (40 ng/mL) plus linear anti-TNF-α peptide (800 μg/mL); TNF-α+TBSP200: TNF-α (40 ng/mL)+tetra-branched scramble peptide (200 μg/ mL); TNF-α+TBTP25: TNF-α (40 ng/mL)+tetra-branched anti-TNF-α peptide (25 μg/ mL); TNF-α+TBTP50: TNF-α (40 ng/mL)+tetra-branched anti-TNF-α peptide (50 μg/ mL); TNF-α+TBTP100: TNF-α (40 ng/mL)+tetra-branched anti-TNF-α peptide (100 μg/ mL); TNF-α+TBTP200: TNF-α (40 ng/mL)+tetra-branched anti-TNF-α peptide (200 μg/ mL); TNF-α+TBTP400: TNF-α (40 ng/mL)+tetra-branched anti-TNF-α peptide (400 μg/ mL)

Characterization of Tetra-Branched Anti-TNF-α-Peptide-Conjugated CAN-γ-Fe_2O_3 NPs

The neat CAN-γ-Fe_2O_3 NPs has an average DLS size of 45.8 nm, and every 10% peptides conjugated to the NPs increased around 5 nm to the DLS diameter of the NPs. The neat CAN-γ-Fe_2O_3 NPs has an average ζ potential of +48 mV, and every 10% peptides conjugated to the NPs reduced approximally 5 mV of ζ potential (Table 2, Figure 4).

NPs	DLS (nm)	ζ potential (mV)
CAN-γ-Fe_2O_3	45.8	+48.0
0310A10% -CAN-γ-Fe_2O_3	49.68	+43.8
0310A50% -CAN-γ-Fe_2O_3	70.63	+24.8

CAN-γ-Fe_2O_3: neat NPs without peptide conjugation; $0310A_{10\%}$ -CAN-γ-Fe_2O_3: covalent contact of tetra-branched anti-TNF-α peptide at 10%wt ratio with CAN-γ-Fe_2O_3 NPs; $0310A_{50\%}$ -CAN-γ-Fe_2O_3: covalent contact of tetra-branched anti-TNF-α peptide at 50%wt ratio with CAN-γ-Fe_2O_3 NPs

Table 2: DLS and ζ potential results for neat CAN-γ-Fe_2O_3 NPs ($Ce^{3/4+}$)-doped maghemite (γ-Fe_2O_3) and peptide-conjugated NPs

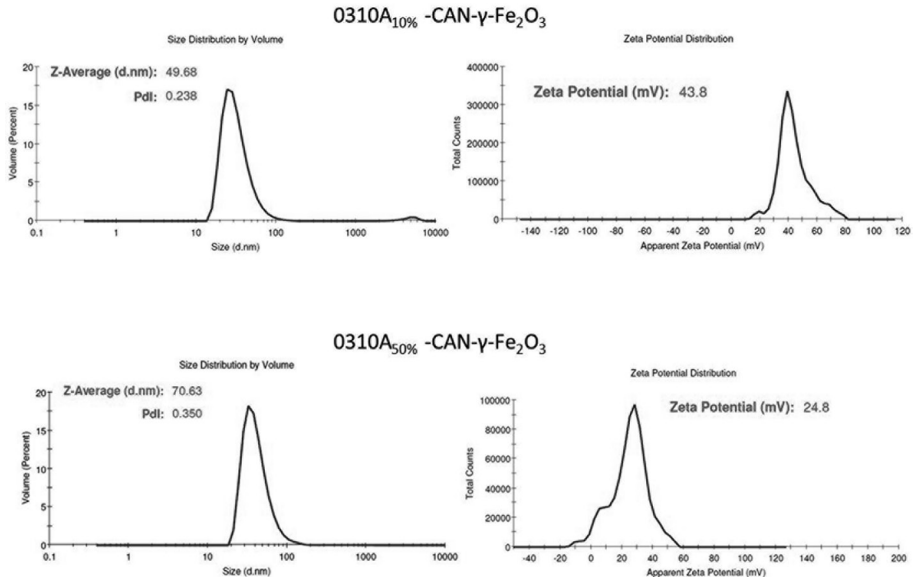

Figure 4: DLS and ζ potential results for neat CAN-γ-Fe_2O_3 NPs ($Ce^{3/4+}$)-doped maghemite (γ-Fe_2O_3 and peptide-conjugated NPs. $0310A_{10\%}$ -CAN-γ-Fe_2O_3: covalent contact of tetra-branched anti-TNF-α peptide at 10%wt ratio with CAN-γ-Fe_2O_3 NPs; $0310A_{50\%}$ -CAN-γ-Fe_2O_3: covalent contact of tetra-branched anti-TNF-α peptide at 50% wt ratio with CAN-γ-Fe_2O_3 NPs

Dynamic Distribution of Tetra-Branched Anti-TNF-Peptide-Conjugated CAN-γ-Fe_2O_3 NPs in Rat Inner Ear Shown by MRI

Significant morphological changes were detected in rat inner ear at 3 h through 2 w post-middle ear administrations of tetra-branched anti-TNF-α-peptide-conjugated CAN-γ-Fe_2O_3 NPs at 10% peptide ratio, which demonstrated that area of the ipsilateral cochlea basal turn, vestibule including the ampulla of semicircular canals shrinked in comparison to the contralateral ear (Figure 5). The changes were most pronounced at 2 w after administration, with typical wiping out of the perilymphatic spaces in the basal turn and hook region of the cochlea, and vestibule (Figure 6). This phenomenon was verified by injection of superparamagnetic iron oxide nanoparticles hierarchically coated with oleic acid and Pluronic® F127 copolymers into the scala tympani of rats. The

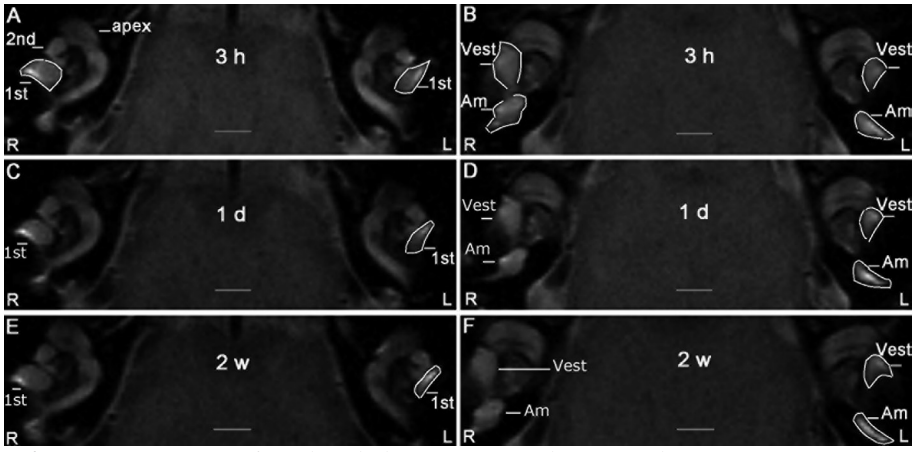

Figure 5: Efficient rat inner ear entry of tetra-branched anti-TNF-α-peptide-conjugated CAN-γ-Fe_2O_3 NPs at 10% peptide ratio shown by MRI. The bright area of inner ear fluids in the basal turn of cochlea (1st), vestibule (Vest), and ampulla of semicircular canal on the delivery side (L) were smaller than that on the contralateral side (R) 3 h after administration, which progressed one day later (1 d) and remained stable in 2 w. **A:** Cochlear MRI at 3 h after administration; **B:** Vestibular MRI at 3 h post-administration; **C:** Cochlear MRI on 1 d after administration; **D:** Vestibular MRI on 1 d post-administration; **E:** Cochlear MRI on 2 w after administration; **F:** Vestibular MRI on 2 w post-administration. 2nd: second turn of cochlea; **L**: Left; **R**: Right. Scale bar=1.0 mm

signal in the endolymphatic spaces of the cochlear hook region and vestibule including ampulla became visibly significantly brighter than that in the contralateral side (Figure 6) [15]. Similar morphology was visualized in both inner ears of rats receiving middle ear administration of tetra-branched anti-TNF-α-peptide-conjugated CAN-γ-Fe_2O_3 NPs at 50% peptide ratio. However, no cell population or structure specific distribution of CAN-γ-Fe_2O_3 NPs conjugated to tetra-branched anti-TNF-α peptide was observed (Figure 7).

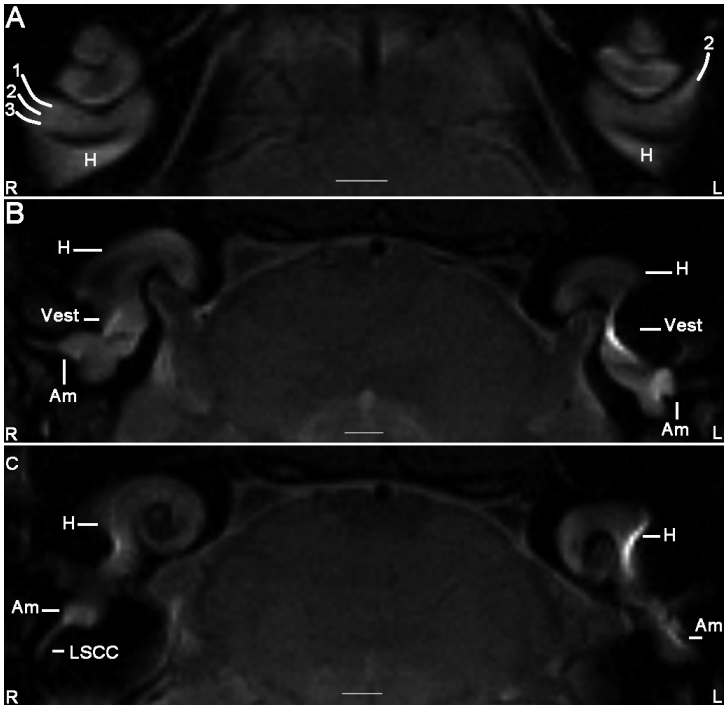

Figure 6: Signal changes in rat inner ear on 1 d post-middle ear administration of tetra-branched anti-TNF-α-peptide-conjugated CAN-γ-Fe_2O_3 NPs at 10% peptide ratio shown by MRI. The narrow strips in the cochlear basal turn and hook region of the delivery ear (L) suggest the scala media **(2)** while the perilymph signal in the scala vestibuli **(1)** and scala tympani **(3)** were wiped out due to distribution of tetra-branched anti-TNF-α-peptide-conjugated CAN-γ-Fe_2O_3 NPs **(A)**. The remnant endolymph signal in vestibule (Vest) **(B)**, ampulla (Am) of the semicircular canal, and hook region of cochlea (H) **(C)** became bright. **LSCC:** Lateral semicircular canal; **L**: Left; **R**: Right. Scale bar=1.0 mm

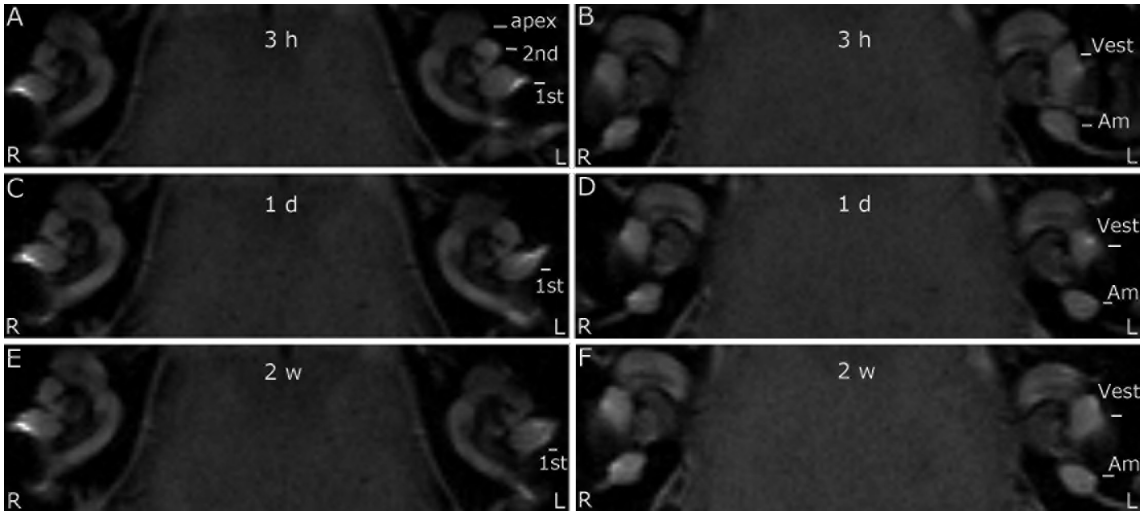

Figure 7: Insignificant rat inner ear entry of tetra-branched anti-TNF-α-peptide-conjugated CAN-γ-Fe_2O_3 NPs at 50% peptide ratio shown by MRI. The cochlea and vestibule (Vest) showed symmetric images on both the delivery (L) and contralateral (R) sides at the time points of 3 h **(A, B)**, 1 d **(C, D)** and 2 w **(E, F)**. Am: ampulla of the semicircular canal; 1st: basal turn of cochlea; 2nd: second turn of cochlea; **L**: Left; **R**: Right. Scale bar=1.0 mm

Inner ear distributions of tetra-branched anti-TNF-α-peptide-conjugated CAN-γ-Fe_2O_3 NPs were histologically detected using Prussian blue staining (Figure 8 and 9). In accordance with the MRI results, CAN-γ-Fe_2O_3 NPs conjugated to tetra-branched anti-TNF-α peptide at 50% peptide ratio did not sufficiently enter the inner ear (Figure 9).

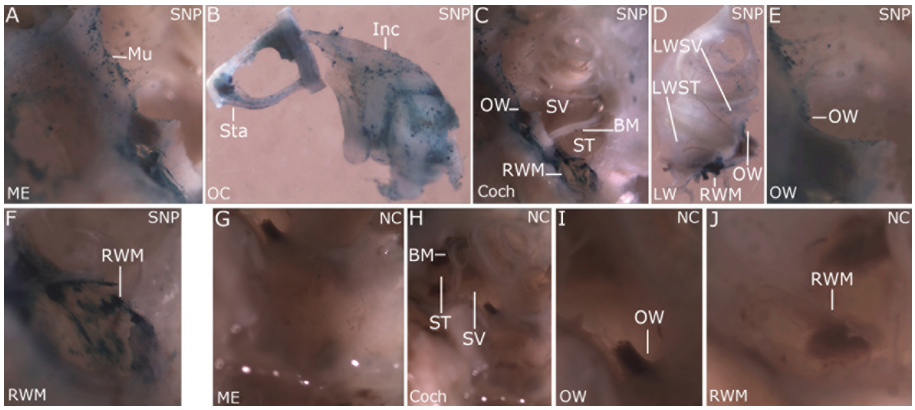

Figure 8: Middle and inner ear distributions of tetra-branched anti-TNF-α-peptide-conjugated CAN-γ-Fe_2O_3 NPs at 10% peptide ratio post-transtympanic injection shown by Prussian blue staining and light microscopy. **BM**: Basilar membrane of cochlea; **Coch**: Cochlea; **Inc**: Incus; **LWST**: Lateral wall of the scala tympany; **LWSV**: Lateral wall of the scala vestibuli; **ME**: Middle ear; **Mu**: Mucosa; **NC**: Negative control; **OC**: Ossicular chain; **OW**: Oval window; **RWM**: Round window membrane; **SNP**: Superparamagnetic nanoparticle; **ST**: Scala tympani; **Sta**: Stapes; **SV**: Scala vestibuli

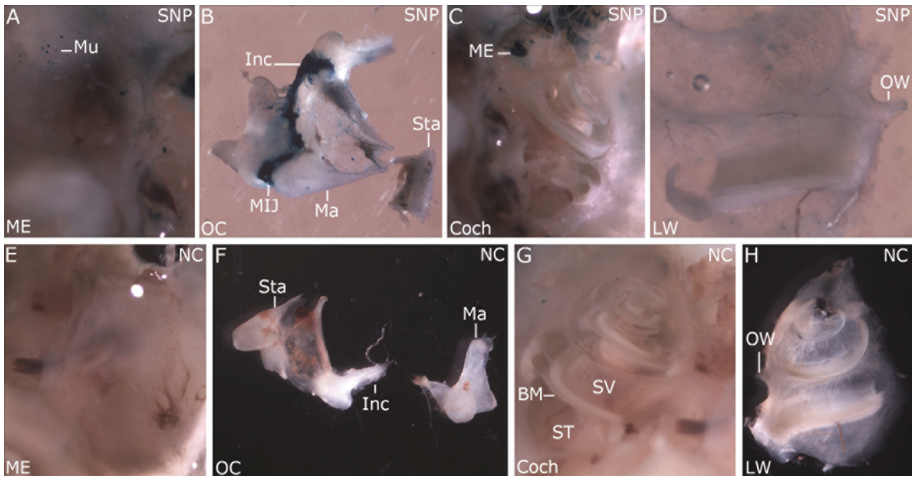

Figure 9: Insufficient inner ear entering of tetra-branched anti-TNF-α-peptide-conjugated CAN-γ-Fe_2O_3 NPs at 50% peptide ratio post-transtympanic injection shown by Prussian blue staining and light microscopy. **BM**: Basilar membrane of cochlea; **Coch**: Cochlea; **Inc**: Incus; **Ma**: Malleus; **ME**: Middle ear; **MIJ**: Malleus-incus joint; **Mu**: Mucosa; **NC**: Negative control; **OC**: Ossicular chain; **OW**: Oval window; **RWM**: Round window membrane; **SNP**: Superparamagnetic nanoparticle; **ST**: Scala tympani; **Sta**: Stapes; **SV**: Scala vestibuli

Discussion

The present study demonstrated that the tetra-branched anti-TNF-α peptide significantly inhibited apoptosis in HUVECs induced by TNF-α, with an inhibitory effect that was significantly greater than did the linear anti-TNF-α peptide. Both *in vivo* MRI and histology displayed that CAN-γ-Fe_2O_3 NPs conjugated to tetra-branched anti-TNF-α peptide at peptide ratio of 10% but not 50% efficiently entered the inner ear and distributed mainly in the perilymphatic spaces after administration in rat middle ear. It indicated that the previously reported novel CAN-γ-Fe_2O_3 NPs had the capacity to carry the novel tetra-branched anti-TNF-α peptide from middle ear into the inner ear [13]. It is possible that the tetra-branched anti-TNF-α peptides are able to pass the middle-inner ear barriers and enter the inner ear by themselves, however, conjugating the peptides onto CAN-γ-Fe_2O_3 NPs endowed the tetra-branched anti-TNF-α peptide a characteristic of visibility by MRI that will be potentially used as a theranostics agent.

In the *in vitro* study, the tetra-branched anti-TNF-α peptide almost fully suppressed the inhibitory effect on HUVECs induced by TNF-α while the linear anti-TNF-α peptide reduced less than half of the TNF-α effect (Figure 5). The branched anti-TNF-α peptide was proven to inhibit TNF-α binding to human melanoma cells expressing TNF-α receptors. However, protecting effect of the tetra-branched anti-TNF-α peptide on cells against TNF-α receptor signaling activation has not been reported before [10]. TNF-α-specific peptide synthesized in linear and tetrameric form showed practically the same binding kinetics to human TNF-α [10]. The tetra-branched anti-TNF-α peptide supressed the TNF-α-induced apoptosis in HUVECs more efficiently than did the linear one might be interpreted as following. The TNF-α-specific peptide and TNF-α receptor may bind to human TNF-α at different sites, and the TNF-α-specific peptide-complexed human TNF-α retains the affinity to TNF-α-receptor; the tetra-branched anti-TNF-α peptide has larger spatial volume than the linear one due to the 3-dimentional conformation, and has higher possibility to block the

TNF-α-receptor binding site on the human TNF-α. The present work provided data showing that the novel tetra-branched anti-TNF-α peptide has potential to be applied in the clinic treatment of diseases associated with TNF-α receptor signaling activation.

In vivo tracking of the tetra-branched anti-TNF-α peptide will provide information on dynamics of the novel peptides in the inner ear, which is a critical issue with respect to quality control of therapeutic study. The novel CAN-γ-Fe_2O_3 NP are a strong T_2-contrast agent attributed by superparamagnetic effect and provides an ideal tool to track the kinetics of therapeutics in the inner ear especially the perilymph and endolymph that are the major buffering systems of the inner ear [13]. The present experiment showed that tetra-branched anti-TNF-α peptide accumulated in the inner ear maximally 1 d after middle ear administration and remained inplace for at least 2 w. The kinetics of CAN-γ-Fe_2O_3 NPs conjugated to tetra-branched anti-TNF-α peptide at a peptide ratio of 10% demonstrated to be significantly slower than that of neat CAN-γ-Fe_2O_3 NPs [13]. This further indicated that the observed dynamic distribution of CAN-γ-Fe_2O_3 NPs in rat inner ear represented the kinetics of tetra-branched anti-TNF-α peptide rather than the behavior of neat CAN-γ-Fe_2O_3 NPs.

Conclusion

In conclusion, the present study demonstrated that the tetra-branched anti-TNF-α peptide reduced apoptosis in HUVECs induced by TNF-α more efficiently than did the linear one. CAN-γ-Fe_2O_3 NPs conjugated to tetra-branched anti-TNF-α peptide at a peptide ratio of 10% but not 50% efficiently entered the inner ear and distributed in the perilymphatic spaces after administration in rat middle ear. It suggested that the previously reported novel CAN-γ-Fe_2O_3 NPs have the capacity to carry the novel tetra-branched anti-TNF-α peptide from middle ear into the inner ear. Coordinately conjugating the peptides onto CAN-γ-Fe_2O_3 NPs endowed the tetra-branched anti-TNF-α peptide a characteristic of visibility by MRI that will be potentially used as a theranostics agent. The present study therefore significantly broadened the application of both the novel peptide and CAN-γ-Fe_2O_3 NPs.

Acknowledgements

The authors thank Yong Xiong for his participating in high performance liquid chromatography of the peptides. This study was supported by China-EU collaborative project sponsored by Ministry of Science and Technology of China (contract grant number: 0102013DFE33160).

Ethical Approval

All applicable international, national, and/or institutional guidelines for the care and use of animals were followed.

References

1. Fujioka M, Kanzaki S, Okano HJ, Masuda M, Ogawa K, Okano H (2006) Proinflammatory cytokines expression in noise-induced damaged cochlea. J Neurosci Res 83: 575-83.

2. Tan WJ, Thorne PR, Vlajkovic SM (2016) Characterisation of cochlear inflammation in mice following acute and chronic noise exposure. Histochem Cell Biol 146: 219-30.

3. Ren J, Li H, Lu Y (1998) [The determinations of tumor necrosis factor and interleukin 6 in serum of patients with sudden sensorineural hearing loss]. Lin Chuang Er Bi Yan Hou Ke Za Zhi 12: 311-3.

4. Demirhan E, Eskut NP, Zorlu Y, Cukurova I, Tuna G, et al. (2013) Blood levels of TNF-alpha, IL-10, and IL-12 in idiopathic sudden sensorineural hearing loss. Laryngoscope 123: 1778-81.

5. Distler GI (1972) Investigation of the properties of the solid-state structure by decoration methods. Bull Acad Sci USSR Phys Ser 36: 1846.

6. Fernandes A, Falcao AS, Silva RF, Gordo AC, Gama MJ, et al. (2006) Inflammatory signalling pathways involved in astroglial activation by unconjugated bilirubin. J Neurochem 96: 1667-79.

7. Van Wijk F, Staecker H, Keithley E, Lefebvre PP (2006) Local perfusion of the tumor necrosis factor alpha blocker infliximab to the inner ear improves autoimmune neurosensory hearing loss. Audiol Neurootol 11: 357-65.

8. Derebery MJ, Fisher LM, Voelker CC, Calzada A (2014) An open label study to evaluate the safety and efficacy of intratympanic golimumab therapy in patients with autoimmune inner ear disease. Otol Neurotol 35: 1515-21.

9. Arpornchayanon W, Canis M, Ihler F, Settevendemie C, Strieth S (2013) TNF-alpha inhibition using etanercept prevents noise-induced hearing loss by improvement of cochlear blood flow in vivo. Int J Audiol 52: 545-52.

10. Brunetti J, Lelli B, Scali S, Falciani C, Bracci L, et al. (2014) A novel phage-library-selected peptide inhibits human TNF-alpha binding to its receptors. Molecules 19: 7255-68.

11. Zou J, Zhang W, Poe D, Zhang Y, Ramadan UA, et al. (2010) Differential passage of gadolinium through the mouse inner ear barriers evaluated with 4.7T MRI. Hear Res 259: 36-43.

12. Haviv AH, Greneche JM, Lellouche JP (2010) Aggregation control of hydrophilic maghemite (gamma-Fe2O3) nanoparticles by surface doping using cerium atoms. J Am Chem Soc 132: 12519-21.

13. Zou J, Ostrovsky S, Israel LL, Feng H, Kettunen MI, et al. (2016) Efficient penetration of ceric ammonium nitrate oxidant-stabilized gamma-maghemite nanoparticles through the oval and round windows into the rat inner ear as demonstrated by MRI. J Biomed Mater Res B Appl Biomater 105: 1883-91.

14. Zou J, Yoshida T, Ramadan UA, Pyykko I (2011) Dynamic enhancement of the rat inner ear after ultra-small-volume administration of Gd-DOTA to the medial wall of the middle ear cavity. ORL J Otorhinolaryngol Relat Spec 73: 275-81.

15. Zou J, Zhang W, Poe D, Qin J, Fornara A, et al. (2010) MRI manifestation of novel superparamagnetic iron oxide nanoparticles in the rat inner ear. Nanomedicine (Lond) 5: 739-54.